JOURNAL OF AGRICULTURAL AND FOOD CHEMISTRY

Article

pubs.acs.org/JAFC

Defensive Armor of Potato Tubers: Nonpolar Metabolite Profiling, Antioxidant Assessment, and Solid-State NMR Compositional Analysis of Suberin-Enriched Wound-Healing Tissues

Keyvan Dastmalchi,[†] Linda Kallash,[†] Isabel Wang,[†] Van C. Phan,[†] Wenlin Huang,[†] Olga Serra,[‡] and Ruth E. Stark*[,†]

[†]Department of Chemistry, The City College of New York, City University of New York Graduate Center and Institute for Macromolecular Assemblies, New York, New York 10031, United States

Department of Natural Sciences, Hostos Community College, 500 Grand Concourse, Bronx, New York 10451, United States

[‡]Laboratori del Suro, Departament de Biologia, Facultat de Ciències, University of Girona, Campus Montilivi s/n, Girona, E-17071 Spain

Supporting Information

ABSTRACT: The cultivation, storage, and distribution of potato tubers are compromised by mechanical damage and suboptimal healing. To investigate wound-healing progress in cultivars with contrasting russeting patterns, metabolite profiles reported previously for polar tissue extracts were complemented by GC/MS measurements for nonpolar extracts and quantitative ^{13}C NMR of interfacial solid suspensions. Potential marker compounds that distinguish cultivar type and wound-healing time point included fatty acids, fatty alcohols, alkanes, glyceryl esters, α,ω-fatty diacids, and hydroxyfatty acids. The abundant long-chain fatty acids in nonpolar extracts and solids from the smooth-skinned Yukon Gold cultivar suggested extensive suberin biopolymer formation; this hypothesis was supported by high proportions of arenes, alkenes, and carbonyl groups in the solid and among the polar markers. The absence of many potential marker classes in nonpolar Atlantic extracts and interfacial solids suggested a limited extent of suberization. Modest scavenging activities of all nonpolar extracts indicate that the majority of antioxidants produced in response to wounding are polar.

KEYWORDS: *Solanum tuberosum, closing layer, wound periderm, solid-state NMR, GC/MS, potential markers, $ABTS^{\bullet+}$ scavenging activity, suberin*

INTRODUCTION

Potatoes can be wounded at various stages during cultivation, collection, storage, and distribution. In the absence of proper healing, the tuber surfaces are vulnerable to desiccation and bacterial infection, which can lead to significant crop losses.[1] Protection is conferred by a wide range of small-molecule metabolites and by the biopolymer suberin, which is deposited at the apoplastic barrier either during plant development or in response to wounding stress.[2,3] Analysis of depolymerization products has produced suberin structural models that include a polyphenolic domain of hydroxycinnamic acid derivatives and monolignols derived from the phenylpropanoid pathway[4,5] as well as a polyaliphatic domain (polyester) with long-chain α,ω-diacids and ω-hydroxyacids, together with glycerol, that are thought to be esterified to the polyphenolic domain by ferulic acid.[6,7] The customary "top-down" approach involves depolymerization of suberized cell walls by chemical treatments and study of the resulting breakdown products to deduce the molecular constituents that comprise the suberin biopolymer. However, limitations of this technique include the incompleteness of depolymerization treatments and their inability to release all classes of chemical constituents, leaving gaps in our understanding of the macromolecular assembly of the suberin macromolecular composite. A potent complementary "bottom up" strategy for understanding potato tuber defense via suberization monitors formation of wound-induced metabolites in potato tissues. This latter approach is also attractive because the cells can be induced synchronously,[8] and the response in the parenchymatic tissue below the wounding surface is initially restricted to those cells that form the closing layer and later to the cells below that form the wound periderm emerging from a new cork cambial layer.[9,10] In this way, changes in the soluble metabolite profile and deposited suberin can be monitored progressively to build an understanding of how the protective biopolymer is formed.

To augment GC/MS metabolite profiling reported for wound-induced tissues from the Russet Burbank potato,[8,11] we recently carried out LC−MS analyses of polar extracts from wound tissues of four potato cultivars with differing patterns of skin russeting (Table 1).[12] These polar metabolomic analyses, conducted for Norkotah Russet, Atlantic, Chipeta, and Yukon Gold cultivars at two developmental time points after wounding, were made in parallel with radical scavenging assays using the 2,2′-azinobis-(3-ethylbenzothiazoline-6-sulfonic acid ammonium salt) free radical ($ABTS^{\bullet+}$).[12] To construct a more

Received: March 18, 2015
Revised: July 9, 2015
Accepted: July 13, 2015
Published: July 13, 2015

DOI: 10.1021/acs.jafc.5b03206
J. Agric. Food Chem. 2015, 63, 6810−6822

Table 1. Potato Cultivars for Metabolite Profiling Studies

cultivar	flesh	periderm russeting	skin
Norkotah Russet	white	russeted and netted	dark tan
Atlantic	white	lightly netted to heavily scaled	white
Chipeta	white	small russeted areas	light to buff
Yukon Gold	light yellow	smooth, finely flaked, yellowish white	yellowish

comprehensive chemical picture of the wound-healing process and its dependence on potato variety, the current study draws on a concurrent partitioning strategy to add cultivar-specific differences in the metabolite profiles and scavenging abilities of nonpolar extracts as well as chemical compositions of the corresponding insoluble material that remains after polar and nonpolar metabolite extraction. Contrasts are also drawn between the metabolites and solid materials present at early (day 3) vs late (day 7) time points after wounding, representing formation of the suberized closing layer as an initial healing response and when the nascent wound periderm is developing, respectively.[9,10,12] The nonpolar compounds signifying those metabolites that distinguish the two wound-healing time points (day 3 vs day 7 in all cultivars) or that discriminate among the four cultivars (at a given time point) are referred to as potential wound-healing and potential cultivar markers, respectively. These compounds were detected using multivariate statistical analysis, then identified and elucidated by matching their GC/MS data with suitable databases. Knowledge of the marker compounds involved in the wound healing process can guide the design of methods to expedite this process, thus improving crop protection during growth and after harvesting. Taken together, these studies can promote the development of food staples possessing beneficial antioxidant capabilities, robust wound healing, and reduced agricultural waste.

MATERIALS AND METHODS

Reagents. The following chemicals were used for extraction and GC/MS analysis: HPLC−MS grade water, methanol, and chloroform (J. T. Baker, Phillipsburg, NJ); hexadecyl hexadecanoate, C_7−C_{40} saturated alkane standards, and formic acid (Sigma-Aldrich, St. Louis, MO); GC/MS grade *N*-methyl-*N*-(trimethylsilyl)trifluoroacetamide (MSTFA) + 1% trimethylchlorosilane (TMCS) (Thermo Scientific, Bellefonte, PA); pyridine (EMD Millipore Corporation, Billerica, MA). Potassium peroxosulfate (Sigma-Aldrich), 2,2′-azinobis (3-ethylbenzothiazoline-6-sulfonic acid ammonium salt) (ABTS), and 6-hydroxy-2,5,7,8 tetramethylchromane-2-carboxylic acid (TCI, Tokyo, Japan) were used for the antioxidant assay.

Plant Material. Potato tuber cultivars from the 2011 crop year were provided by Joe Nuñez, University of California Cooperative Extension (Davis, CA). Differences in their overall phenotypic characteristics are summarized in Table 1.

Sample Preparation. The dormant freshly harvested potato tubers were peeled, sectioned, and allowed to heal as described previously.[12] Briefly, internal flesh tissues were sectioned longitudinally with a mandolin slicer to obtain disks about 5 mm thick. Healing in the dark at 25 °C was accomplished by placing the slices on wet cellulose filter paper inside closed humidified plastic boxes equipped with wire netting supports. The new brown surface layer of wound-healing tissue is identifiable because it is easily excoriated and detached, then removed by sweeping a flat spatula under the layer. During tissue collection, flesh (parenchyma) contamination under the wound healing surface was avoided to the extent possible. The samples were harvested at 3 and 7 days after wounding, corresponding to early healing in which the suberized closing layer had formed and to the developing wound periderm, respectively. Samples were frozen immediately in liquid nitrogen and stored at −80 °C. Processing involved grinding under liquid nitrogen, freeze-drying, and again storing at −80 °C.

For chemical analysis, concurrent extraction and partitioning of polar and nonpolar constituents were carried out using a slightly modified version of the method introduced by Choi et al.[13] for metabolomics of plant materials.[14] Extraction of 10 mg samples by 1 min of pan ultrasonication (Branson Ultrasonics, Danbury, CT) in 2 mL of 60% (v/v) methanol−water was followed by addition of 2 mL of chloroform and an additional 1 min of sonication in a 4-mL glass vial. Extracts were then incubated in a shaker at room temperature for 10 min, followed by tabletop centrifugation (Beckman Coulter, Fullerton, CA) at 1089*g* and 25 °C to produce three phases: upper soluble polar, lower soluble nonpolar, and an interphase of suspended particulates. After removal of the liquid polar and nonpolar extracts with a glass Pasteur pipet, the remaining residue of interfacial particulate solids was filtered, washed, and dried under a flow of nitrogen. Six biological replicates per cultivar were extracted in parallel for each of the day-3 and day-7 time points.

GC/MS Analysis. The samples were prepared according to Yang et al.[8] For metabolite separation and identification, a 500-μL aliquot of each nonpolar extract was placed in a glass vial and evaporated. Each sample was then reconstituted with 50 μL of pyridine and derivatized using 50 μL of *N*-methyl-*N*-(trimethylsilyl) trifluoroacetamide (MSTFA) + 1% trimethylchlorosilane (TMCS) at 50 °C for 1 h. Samples were analyzed with a QP2010 GC/MS (Shimadzu USA, Canby, RI) spectrometer with the injector oven set at 250 °C. The injection mode was splitless, and the volume injected for each sample was 1 μL. A Durabond-5 column (30 m × 0.25 mm i.d., film thickness 0.25 μm; Agilent Technologies, Santa Clara, CA) was used. The temperature program was based on the published method of Yang et al.[8] with minor modifications. After an initial delay of 5 min at 70 °C for the solvent to clear the system, the oven temperature was raised to 310 °C at a rate of 5 °C/min. The oven was kept at this temperature for 11 min and allowed to cool afterward to 70 °C. A 1-μL injection of 0.3 μM hexadecyl hexadecanoate provided a reference standard.

Preprocessing of GC/MS Data. The GC/MS data with a .qgd extension were converted to ANDI (CDFNET) format. MZmine version 2.4 (VTT Technical Research Center, Helsinki, Finland and Turku Center for Biotechnology, Turku, Finland) that included filtration, deconvolution, peak alignment, and data normalization was used for processing.[15] The region between 0 and 15 min, which contains peaks from derivatization artifacts, was excluded from the analysis. These peaks were also observed in blanks consisting of the solvent, pyridine, and derivatization reagent.

Multivariate Statistical Analysis. Simca-P+ software version 13.0 (Umetricas, Umea, Sweden) was used to carry out principal component analysis (PCA) of GC/MS data processed with MZ Mine using Pareto scaling.[16] This method organizes the data by relating the observations, cultivar types, and variables of the LC−MS data. The method tests the consistency of each set of biological replicates and discriminates among the different sample types.

Orthogonal partial least-squares discriminate analysis (OPLS-DA) of the data followed by the generation of S-plots helped to identify compounds that account for the differences among cultivars and between different wounding time points, which were designated as potential cultivar and potential wound-healing markers, respectively (Supporting Information, Figure S1). OPLS-DA is a regression and prediction method that finds information in the X data (e.g., variables from the LC−MS experiments) that is related to information in the Y data (e.g., discrete variables specifying cultivar type or wound-healing time point). This method shows how these two sets of information vary together and if they are dependent on each other, facilitating classification studies and potential marker identification. The S-plot serves to visualize OPLS-DA results in a scatter plot.[17] The variables (e.g., MS ions) at the extreme ends of the S-plot had $p(\mathrm{corr})\,[1] > 0.8$, indicating high reliability;[17] they were further examined using a variable line plot to check how specific they were to the sample type and if they qualified as potential marker ions (Supporting Information, Figure S1).

DOI: 10.1021/acs.jafc.5b03206
J. Agric. Food Chem. 2015, 63, 6810−6822

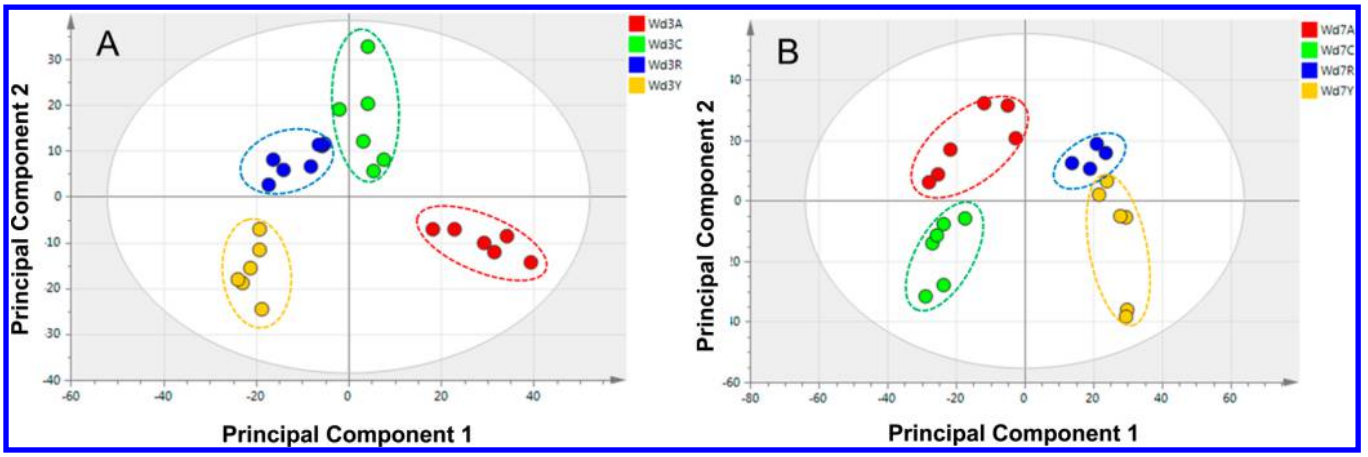

Figure 1. PCA score plot of GC/MS data from nonpolar extracts, showing consistency of each set of biological replicates and discrimination among the differently russeted cultivars at each of two time points after wounding. Included are wound-healing samples at day 3 (Wd3, A), and day 7 (Wd7, B), designated as Atlantic (red, A), Chipeta (green, G), Norkotah Russet (blue, R), and Yukon Gold (gold, Y) cultivars. The *x* and *y* axes of the plots represent the score values of principal components 1 and 2, respectively.

The PCA model was validated by calculating the values of R^2 and Q^2, which indicate fitness and predictive ability, respectively.[16] The Q^2 value, which is reported as a result of cross validation of the model, exceeded 0.5.[17] Cross validation using SIMCA-P+ divided the data into seven groups, one of which was removed. The model was then generated with the remaining groups, and the deleted group was predicted by the model. The partial predictive residual sum of squares (PRESS) was calculated. This procedure was repeated seven times to sum the partial PRESS values, obtain the overall PRESS, and calculate the Q^2 value. R^2 was larger than Q^2, but the difference between R^2 and Q^2 was small, as recommended.[17] For OPLS-DA, in addition to Q^2, the model diagnostics included R^2X and R^2Y values calculated for the X and Y variables, respectively.[17]

Metabolite Structural Identification. The ions corresponding to markers and other metabolites were identified using the Wiley Library (9th edition/NIST 2008). The ionic spectrum of each metabolite was matched against the spectra of known compounds from the library using a similarity index to identify hits. In addition, the observed spectra were compared with those of the known compounds for the ratio of ion intensities. C7−C40 saturated alkane standards (Sigma-Aldrich, St. Louis, MO) were injected. On the basis of their retention times and m/z values and using the NIST library peaks, they were assigned to standard reference compounds. There is a direct correlation between retention time and chain length.

$ABTS^{\bullet+}$ Scavenging. Antioxidant assessment of the nonpolar extracts was conducted using an $ABTS^{\bullet+}$ scavenging assay essentially as described by Dastmalchi et al.[12] Reaction of an aqueous ABTS solution (7 mM) with $K_2S_2O_8$ (2.45 mM) in the dark for 12−16 h at room temperature yielded $ABTS^{\bullet+}$, for which the absorbance at 734 nm was adjusted to 0.70 (±0.02) with ethanol. To a 2-μL aliquot of the extract of interest was added 198 μL of the $ABTS^{\bullet+}$ reagent; the absorbance at 734 nm was monitored after initial mixing and at 5 min intervals up to 45 min using a $Spectra_{max}$ M5 microplate reader (Molecular Devices, Sunnyvale, CA). Each percentage inhibition value was calculated as

$$\frac{Abs_{control} - Abs_{sample}}{Abs_{control}} \times 100$$

A calibration plot of percentage inhibition versus concentration was made for the reference standard, 6-hydroxy-2,5,7,8-tetramethylchroman-2-carboxylic acid (Trolox), permitting calculation of the Trolox equivalent antioxidant capacity (TEAC, mmol Trolox/g dried sample) for each extract.

Isolation of Suberin-Enriched Tissues. The interfacial solid from the partitioned mixture was passed through a Whatman no. 4 filter paper and then washed with distilled water. To remove unsuberized cell-wall materials, the sample was treated with 0.1% (w/v) *Aspergillus niger* cellulase (MP Biomedicals, Illkirch, France) in a 50 mM pH 5.0 acetate buffer for 48 h each at 37 and 44 °C, respectively. The residue was then treated with 0.4% (v/v) *A. niger* pectinase (Sigma-Aldrich) in a 50 mM pH 4.0 acetate buffer for 24 h each at 28 and 31 °C, respectively. After the enzyme treatments, the sample was filtered, washed with deionized water, and dried at 50 °C. Soxhlet extraction was conducted under reflux conditions to remove any remaining waxes and soluble lipids, using a succession of solvents of varying polarity: methanol, chloroform, and hexane for 48 h each. The resulting solid suberin-enriched samples were reserved for solid-state NMR analysis.

Solid-State NMR Analysis. The chemical moieties present in the suberin-enriched materials were identified and quantitated using cross-polarization and direct polarization magic-angle spinning ^{13}C NMR experiments (CPMAS, DPMAS) on 3−4 mg powdered samples. A four-channel Agilent (Varian) DirectDrive I (VNMRS) NMR spectrometer (Agilent Technologies, Santa Clara, CA, USA) operating at a ^1H frequency of 600 MHz (^{13}C at 150 MHz) and equipped with a 1.6 mm HXY FastMAS probe operating at a spinning rate of 10.00 kHz (±20 Hz) was used. The spectral data were typically processed with 100 Hz line broadening and analyzed in parallel using VNMRJ (version 2.2C; Agilent) and ACD/NMR Processor Academic Edition (version 12; Advanced Chemistry Development, Inc., Toronto, ON, Canada). Chemical shifts were referenced externally to the methylene ($-CH_2-$) group of adamantane (Sigma-Aldrich) at 38.48 ppm.

For typical CPMAS experiments used to identify the carbon-containing functional groups via their respective chemical shifts, conditions included 90° pulse durations of 1.3 and 1.2 μs for ^1H and ^{13}C, respectively, a contact time of 1.5 ms, acquisition delay of 4 μs, and recycle delay of 3 s between successive acquisitions. Heteronuclear decoupling was applied with a ^1H field strength of 204 kHz using the SPINAL method.[18] The spectral width was 46296 Hz, and the number of transients was 21500. For DPMAS experiments used to estimate the relative proportions of each carbon type, a 100-s recycle delay was used to collect 2600 transients.[19] Alternatively, quantitatively reliable ^{13}C NMR spectra of suberized cell walls were obtained by acquiring 100 transients with the multiple-CPMAS method[20] after validation with a *t*-BOC alanine standard (Sigma-Aldrich) and through DPMAS measurements for the Norkotah Russet day-7 wound suberin. Radiofrequency (rf) fields of ω_{1H} = 204 kHz and ω_{1C} = 189 kHz were used for all 90° pulses. Transfer of polarization from ^1H to ^{13}C nuclei was achieved via the condition $\omega_{1C} - \omega_{1H} = \omega_{rotation}$, with rf frequencies of ω_{1H} = 53.3 kHz and ω_{1C} = 63.4 kHz; a 10% linear ramp of the ^1H radiofrequency power was used during the CP period. Recycle times between successive cross-polarizations were 1.0 s; 11 contact times of 1.0 ms were used to acquire each transient. SPINAL

DOI: 10.1021/acs.jafc.5b03206
J. Agric. Food Chem. 2015, 63, 6810−6822

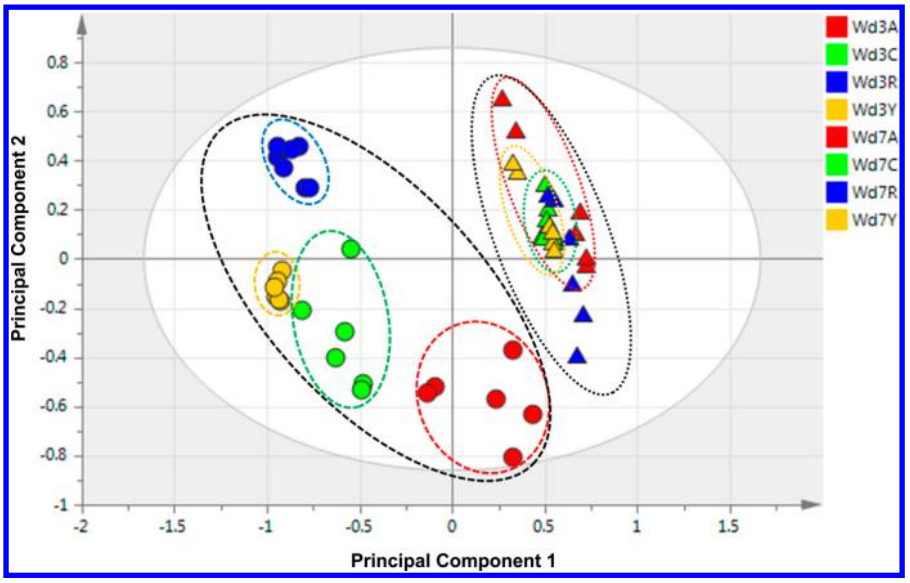

Figure 2. PCA score plot of GC/MS data from nonpolar extracts, showing overall differences among the metabolite profiles for wound-healing samples of four cultivars at day 3 (circles) and day 7 (triangles). The samples are color-coded as Atlantic (red, A), Chipeta (green, C), Norkotah Russet (blue, R), and Yukon Gold (gold, Y) cultivars. The *x* and *y* axes of the plots represent the score values of principal components 1 and 2, respectively.

heteronuclear decoupling[18] with ω_{1H} = 204 kHz was applied during an acquisition period of 22 μs.

The 3-day wound healing samples required 5000 transients (~20 h), whereas 7-day samples required only 1500 transients (~6 h). Integrated signal intensities were measured by counting pixels with the image manipulation software GIMP (www.gimp.org) and using the following chemical shift ranges to denote major structural components of suberin: carboxyl and amide groups (168−180 ppm, region 1); arenes and alkenes (115−160 ppm, region 2); alkoxy groups (96−108, 80−92, 67−80, 59−67 ppm; regions 3−6); methoxy groups (45−59 ppm, region 7); alkyl chain methylenes (15−45 ppm, region 8). Each chemical shift range was extended by ±1 ppm to ensure that the regions were not truncated in the middle of a resonance. Each quoted quantitative estimate was the result of measurements on two biological replicates, quoted as mean ± standard error.

Statistical Analysis. The antioxidant and solid-state NMR data were presented as mean values ± standard error. Significant differences between the values were determined using Tukey's pairwise comparison[21] at a level of $P < 0.05$, assessed with JMP software version 12 (http://www.jmp.com).

RESULTS AND DISCUSSION

GC/MS Multivariate Analysis Reveals Distinctive Metabolite Profiles for the Four Cultivars. The PCA score plots derived from GC/MS of the day-3 nonpolar samples show clear, nonoverlapping clusters representing the respective metabolite profiles of the four cultivars (Figure 1A), but those differences are less distinct for the day-7 time point (Figure 1B). For the GC/MS data considered collectively from both time points, the PCA plot of Figure 2 clearly shows that the cluster corresponding to all of the day-7 extracts is more compact compared with the overall day-3 cluster. This trend, which was also reported for the corresponding polar extracts[12] and for Russet Burbank wound-healing samples,[8] is likely to reflect a common biosynthetic pathway induced by wounding in each of the four cultivars. Thus, similar phytochemicals associated with wound healing are expected to become increasingly dominant with respect to the initially distinct metabolite pools of each cultivar. For the Atlantic extracts, the similar values of the first principal component (PC1) observed for day-3 and day-7 clusters (Figure 2) indicate that its nonpolar metabolites change more modestly, or at a slower rate, in response to wounding.

The nonpolar compounds that distinguish the two wound-healing time points (3-day vs 7-day for all cultivars) or the four cultivars at a particular time point can be considered as potential wound-healing and cultivar markers, respectively. These compounds were identified from the "wings" of S-plots generated by OPLS-DA[12] (Supporting Information, Figure S1) and elucidated structurally by matching their GC/MS data against the spectra of known compounds from the Wiley Library as described above. A total of 28 identified potential marker compounds were detected from the S-plots and variable line plots as noted above.

These compounds were classified as alkanes, α,ω-fatty diacids, α,ω-hydroxyfatty diacids, fatty acids, hydroxyfatty acids, fatty alcohols and aldehydes, and glyceryl esters (Table 2, **1**−**28**). Seven compounds that distinguish the day-7 time point (hentriacontane (**3**, 31:0), 2-hydroxysebacic acid (**8**, 10:0), tetradecanoic (myristic) acid (**10**, 14:0), hexadecanoic (palmitic) acid (**12**, 16:0), heneicosanoic acid (**19**, 21:0), tetracosanoic acid (**21**, 24:0), and pentacosanoic acid (**22**, 25:0)) are referred to as potential wound-healing markers. These compounds, which include an alkane, an α,ω-hydroxyfatty diacid, and several fatty acids, are more abundant at day 7 in all cultivars. Hentriacontane (**3**) has been reported to be cytotoxic to in vitro L5178Y-R lymphoma murine model.[22] Tetradecanoic (**10**, 14:0) and hexadecanoic (**12**, 16:0) acids have been reported to inhibit the growth of phytopathogenic fungi.[23]

By plotting the number of nonpolar potential marker compounds in each structural class by cultivar type and time point (Figure 3), it was possible to discern additional trends and lay the groundwork to align our metabolite findings for the extracts with the solid interfacial layers described below. Whereas most potential cultivar markers are found at day 7 postwounding, when suberin biosynthesis is well underway, nine of the markers are found in day-3 extracts of the various

DOI: 10.1021/acs.jafc.5b03206
J. Agric. Food Chem. 2015, 63, 6810−6822

Table 2. Potential Marker Compounds for Nonpolar Extracts from Potato Wound Tissues of Four Cultivars

Compound Number	Metabolite	C:D[a]	Potential Cultivar Marker[b]	Potential Wound-Healing Marker[c]	Molecular Structure[d]
Alkanes					
1	Heneicosane[e-g]	21:0	Wd7A Wd7C		
2	Triacontane[f,h]	30:0	Wd7Y		
3	Hentriacontane	31:0	Wd7Y	+	
α,ω-Fatty Diacids					
4	Butanedioic acid	4:0	Wd7A Wd7C		
5	Octanedioic acid	8:0	Wd7A		
6	Azelaic acid[e]	9:0	Wd7C Wd7R		
7	Sebacic acid[f]	10:0	Wd7C		
α,ω-Hydroxyfatty Diacids					
8	2-Hydroxysebacic acid[h]	10:0	Wd3C Wd7Y	+	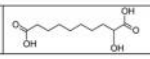
Fatty Acids					
9	Undecanoic acid	11:0	Wd7A Wd7C		
10	Myristic acid/Tetradecanoic acid[f,h]	14:0	Wd7C Wd7R	+	
11	Pentadecanoic acid[f]	15:0	Wd3Y Wd7C Wd7R		
12	Palmitic acid/Hexadecanoic acid[f-h]	16:0	Wd3A Wd3Y Wd7C Wd7Y		
13	Heptadecanoic acid[f,h]	17:0	Wd7A Wd7C		
14	Stearic acid/Octadecanoic acid[f-h]	18:0	Wd3Y Wd7C		
15	Oleic acid/cis-9-octadecanoic acid[f-h]	18:1	Wd7R Wd3C		
16	17-Octadecynoic acid[f]	18:1	Wd3A		
17	9,12-Octadecadienoic acid/Linoleic acid[f-h]	18:2	Wd3R		
18	Eicosanoic acid[f-h]	20:0	Wd7C Wd7R		
19	Heneicosanoic acid[f,g]	21:0		+	
20	Docosanoic acid[f-h]	22:0	Wd7A Wd7C		
21	Tetracosanoic acid[f,g]	24:0	Wd3Y	+	
22	Pentacosanic acid[f]	25:0		+	
Hydroxyfatty Acids					
23	12-hydroxystearic acid	18:0	Wd3C Wd7C		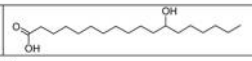
Fatty Alcohols and Aldehydes					
24	cis-hexanedecanal	16:0	Wd7A		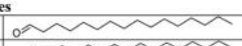
25	Hexadecane-1,2 diol[e-g]	16:0	Wd7C		
26	Oleoyl alcohol/cis-9-octadecenol	18:1	Wd7C		
Glyceryl Esters					
27	Glycerol monopalmitate/monopalmitin[f,h]	19:0	Wd7C Wd7Y		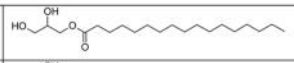
28	Glycerol monostearate[f,h]	21:0	Wd7R Wd7Y		

[a]Alkyl or acyl chain specification, where *C* is the number of carbon atoms and *D* is the number of double bonds. [b]The wounding time points are denoted by Wd3 and Wd7; entries are color coded according to the cultivar for which the potential marker is specific: Atlantic (red), Chipeta (green), Norkotah Russet (blue), and Yukon Gold (gold). For instance, **Wd7Y** for Hentriacontane (**3**, 31:0) designates that compound as a Yukon Gold potential marker in the day-7 nonpolar extract. [c]These entries denote the potential marker compounds that are more abundant in all the four cultivars at day 7, which is associated with the development of the wound periderm. For instance, '+' for Hentriacontane (**3**, 31:0) designates that compound as notably abundant at day 7 for all four cultivars. [d]From the Wiley Library (9th edition/NIST 2008) unless noted otherwise. [e]Detected among the marker compounds identified in native periderms of these four cultivars (Huang et al., unpublished). [f]Yang, W.-L.; Bernards, M. A. Metabolite profiling of potato (*Solanum tuberosum* L.) tubers during wound-induced suberization. *Metabolomics* **2007**, *3*, 147−159. [g]Yang, W.-L.; Bernards, M. A. Wound-induced metabolism in potato (*Solanum tuberosum*) tubers. *Plant Sig. Behav.* **2006**, *1*, 59−66. [h]Detected among the metabolites identified in native periderms of these four cultivars (Huang et al., unpublished).

cultivars. All four Yukon Gold day-3 markers are fatty acids, three of which appear later as day-7 Chipeta markers (Table 2). The largest numbers of fatty acid markers are present at day 3 for Yukon Gold and at day 7 for Chipeta, followed by Norkotah Russet, respectively (Figure 3A). Fatty acids, which can be substrates for subsequent elongation, hydroxylation, or esterification steps during suberin biosynthesis, comprise nearly 40% of the nonpolar potential markers overall. Therefore, we

DOI: 10.1021/acs.jafc.5b03206
J. Agric. Food Chem. 2015, 63, 6810−6822

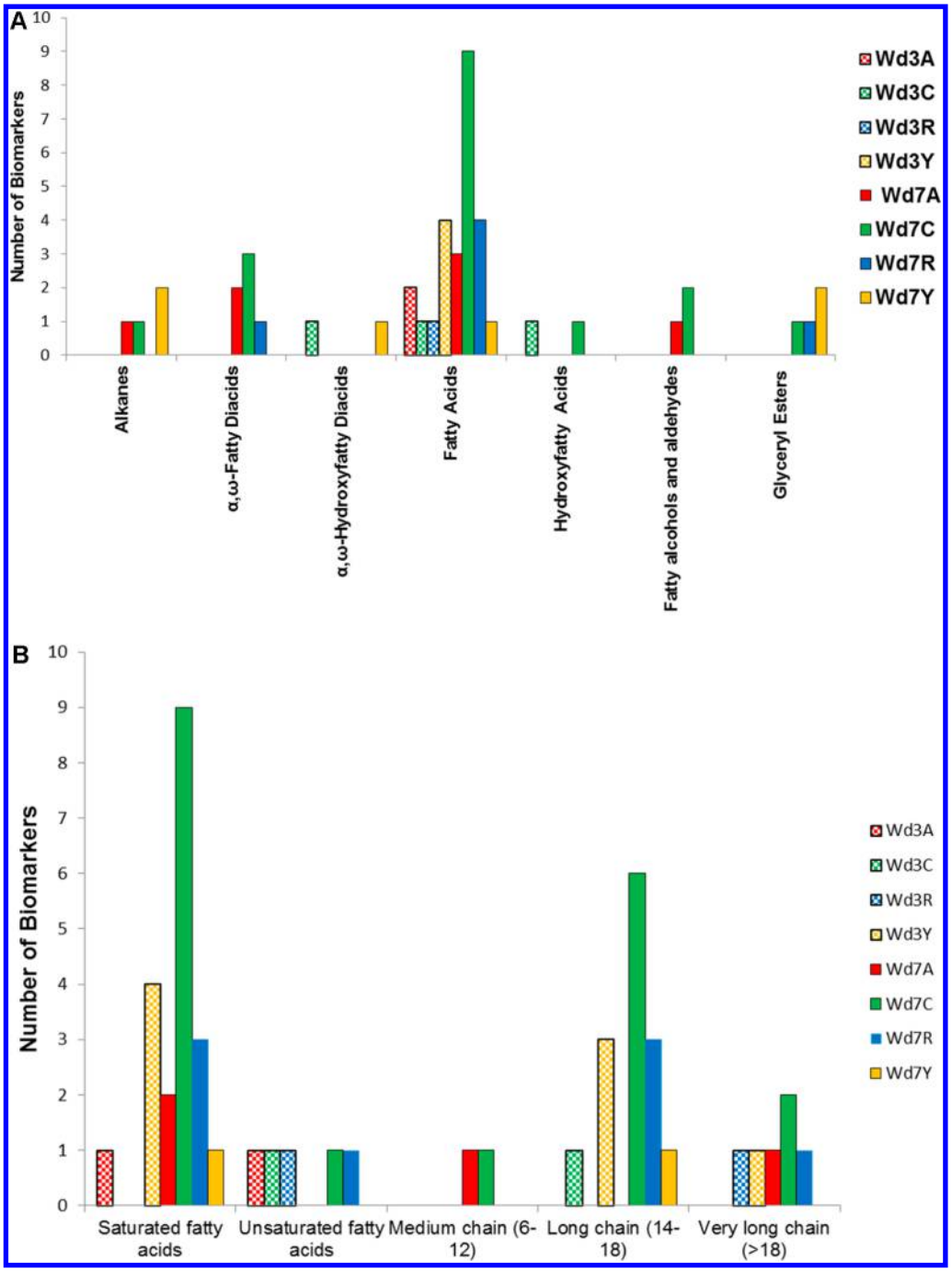

Figure 3. Accumulation of nonpolar marker compounds as a function of chemical class and time point after tissue wounding. (A) Nonpolar markers of day-3 and day-7 potato periderm extracts; (B) a detailed view of the fatty acid potential marker class. The samples are coded for Atlantic (red, A), Chipeta (green, C), Norkotah Russet (blue, R), and Yukon Gold (gold, Y), using checkerboards for day-3 and solid colors for day-7 markers, respectively.

examined this chemical class of markers in greater detail (Figure 3B), finding a significant portion (21%) of unsaturated homologues overall, although none in the Yukon Gold extracts. The fatty acid markers exhibit a broad distribution of chain lengths (11−25), with the majority in the range of 14 to 18 but no clear correlations of length according to healing time point.

The Chipeta cultivar contains nearly all potential marker classes (specifically at the day-7 time point), but a progressively diminished range of these abundant nonpolar metabolites is observed for Yukon Gold, Norkotah Russet, and Atlantic varieties. All Yukon Gold markers are saturated. Each of the less numerous marker classes is absent in one or more cultivars; hydroxyfatty acid and fatty alcohol markers are unique to the Chipeta cultivar at the day-7 time point. The absence of glyceryl ester, hydroxyfatty acid, and α,ω-hydroxyfatty diacid markers in the Atlantic cultivar is notable: the paucity of these key building blocks of suberin[2] could indicate limited development of its protective suberin polymer, particularly if the trend is confirmed in the solid biopolymer (see below).

Given that aliphatic compounds in general and free fatty acids in particular offer protection against fungal (*Fusarium sambucinum*) infections,[10,24] these compounds that have been

DOI: 10.1021/acs.jafc.5b03206
J. Agric. Food Chem. 2015, 63, 6810−6822

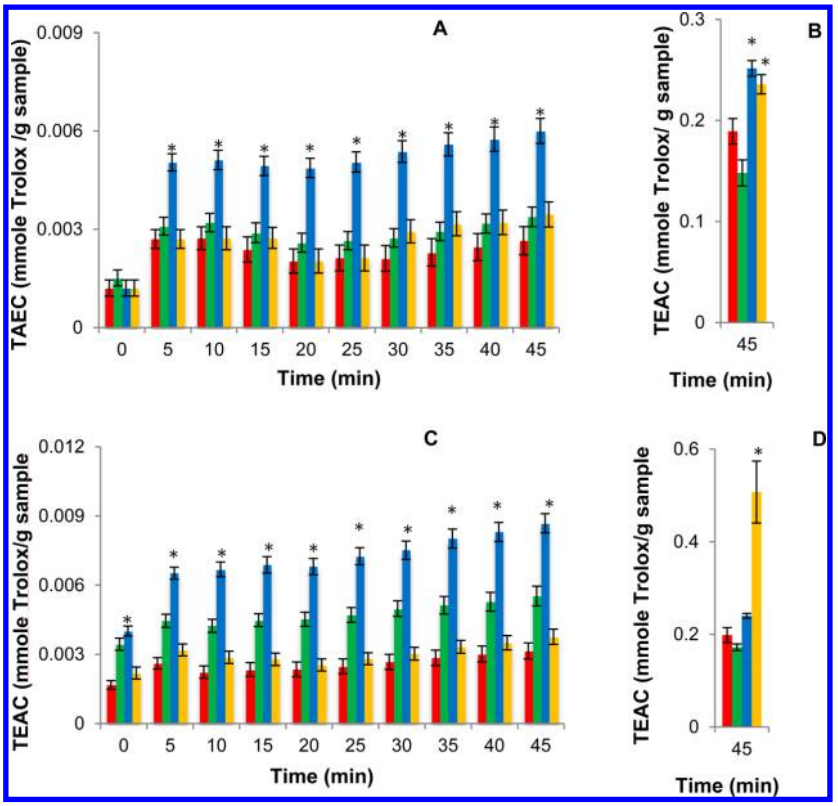

Figure 4. Antioxidant activity throughout the 45 min ABTS assay period for wound-healing potato extracts from Atlantic (red), Chipeta (green), Norkotah Russet (blue), and Yukon Gold (gold) cultivars, showing activities at day-3 post wounding for nonpolar (A) and polar (B) extracts; day-7 postwounding for nonpolar (C) and polar (D) extracts revealing diminished radical scavenging for nonpolar extracts (~50-fold at the 45 min assay time illustrated herein, ~100-fold at the 0 min assay time based on our prior report[12]). Scavenging activities for the nonpolar extracts were examined herein; polar extracts have been reported previously.[12] The data represent the mean ± standard error of the mean of six biological replicates for each cultivar. The highest significant scavenging activity ($P < 0.05$) at each time interval, calculated by means of Tukey pairwise comparisons, is denoted by an asterisk (*).[21]

found abundantly in all cultivars could provide strong protection against fungal infection. Unsaturated fatty acid markers such as 9-octadecenoic acid (oleic acid) (**15**, 18:1) and 9,12-octadecadienoic acid (linoleic acid) (**17**, 18:2) have also been implicated as active compounds against plant pathogenic fungi[25] and may contribute to the antioxidant activities described below.

Diacids such as markers **4**–**8** provide potential sites for the developing suberin biopolymer: for attachment to glycerol forming glyceryl esters, for esterification with long-chain alcohols forming linear esters, or for covalent linkages at either end.[6] Thus, these metabolites can build cross-links within the suberin polyester.[4] All fatty diacid markers emerge in day-7 extracts; namely, at a later time point in the healing process when the wound periderm is developing. Moreover, it is striking that these diacids have relatively short acyl chains compared with native periderm constituents (Huang et al., unpublished). However, medium-chain (C8–C12) species with saturated aliphatic chains have also been reported in wound-healing potato tissues as suberin triglyceride degradation products,[26] in contrast to the typical C16, C18, and longer chain lengths found as suberin monomers.[4,6] One of the diacid markers, 2-hydroxysebacic acid (**8**, 10:0), is up-regulated in all cultivars at day 7 (Table 2). Among the diacid markers, azelaic acid (**6**, 9:0) has been implicated in the plant immune system of *Arabidopsis*, offering protection against pathogens.[27]

Some of the potential markers identified in the current study (Table 2) have been reported previously as metabolites in wound tissue extracts[8] of potato tubers. Those marker compounds reported for the first time in the nonpolar extracts from potato wound tissues included α,ω-fatty diacids (**4**–**7**), an α,ω-hydroxyfatty diacid (**8**, 10:0), a fatty acid (**9**, 11:0), a hydroxyfatty acid (**23**, 18:0), an alcohol (**26**), an aldehyde (**24**, 16:1), and an alkane (**3**, 31:0). Conversely, some longer-chain fatty acid (28:0–30:0) and alcohol (20:0–27:0 and 29:0) metabolites reported previously[8] were not detected in the current study (Supporting Information Table 1). Since our GC/MS protocol successfully detects long-chain metabolites, we attribute this discrepancy to cultivar differences or unintended variations in tissue preparation procedures. Longer chain fatty acids, fatty alcohols, and alkanes have also been found previously in native potato periderms[5,7] (Huang et al., unpublished), but their absence in wound-healing tissues is sensible in light of their well-established anatomical and physiological differences.[28] The identified fatty acids included odd-numbered homologues, which have also been reported previously in the wound tissues of potato tubers[8] and are known elsewhere in the plant kingdom.[29] Some polar compounds, such as phenolic acids, sugars, and amino acids, were found in the nonpolar extracts, presumably as a result of bleed-through effects during the partitioning of the soluble layers.

ABTS$^{\bullet+}$ Scavenging Varies with Cultivar, Time Point, and Extract Polarity. It has been proposed that wounding of potato tubers contributes to the formation of reactive oxygen species and subsequent oxidative stress.[30] Nonetheless, both

DOI: 10.1021/acs.jafc.5b03206
J. Agric. Food Chem. 2015, 63, 6810–6822

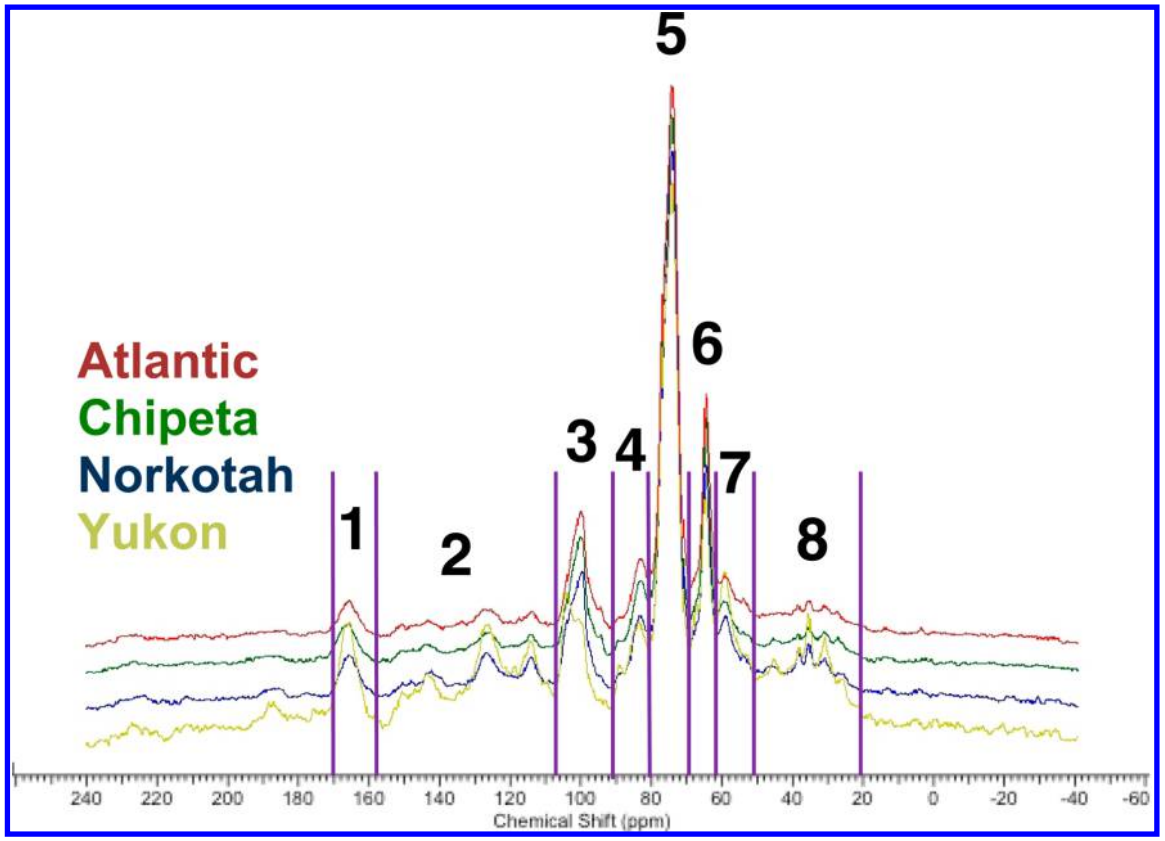

Figure 5. Stacked multi-CP solid-state ^{13}C NMR spectra of representative suberin-enriched tissue samples from each of the four cultivars at the day-7 post wounding time point, showing the chemical moieties present in the solid interfacial layer. The separated regions in the spectra are carboxyl and amide groups (168−180 ppm, region 1); arenes and alkenes (115−160 ppm, region 2); alkoxy groups (96−108, 80−92, 67−80, 59−67 ppm; regions 3−6); methoxy groups (45−59 ppm, region 7); and alkyl chain methylenes (15−45 ppm, region 8). Each spectrum was normalized by setting the largest peak to full scale.

increasing and decreasing stress responses of potato tissues by production of antioxidant chemical compounds have been reported by the same authors in response to wounding.[30,31] To avoid the established limitations of the diphenylpicrylhydrazyl free radical scavenging assay used in prior studies (narrow pH range, steric hindrance, spectral interference),[32,33] we selected an $ABTS^{\bullet+}$ assay. The latter method also permits clean comparisons with our previous investigation[12] of antioxidant activity in polar extracts derived concurrently from the same potato tissue samples. The end result is a more comprehensive picture of antioxidant activity in the potato wound tissues from these four cultivars.

Figure 4 shows that the activities of nonpolar extracts at day 7 postwounding (Figure 4C) are significantly higher than at day 3 postwounding (Figure 4A), supporting an accumulation of antioxidant constituents during the wound-healing process. The order of activity for day-3 nonpolar samples is Norkotah Russet > Chipeta ~ Yukon Gold > Atlantic, whereas at day 7 the trend changes slightly to Norkotah Russet > Chipeta > Yukon Gold ~ Atlantic. Thus, the heavily russeted Norkotah Russet cultivar exhibits the highest scavenging activity for both day-3 and day-7 nonpolar extracts.

As noted above, the applicability of the $ABTS^{\bullet+}$ scavenging assay for antioxidant activity of both polar and nonpolar compounds[32,33] makes it possible to compare the respective data directly. As a group, the antioxidant activities after 45 min of free radical scavenging reaction for both day-3 and day-7 extracts are 50- to 100-fold smaller for the nonpolar samples (Figure 4), reflecting the relative dearth of phenolic and other unsaturated molecular moieties among the nonpolar metabolites. Conversely, it can be deduced that the majority of the antioxidant compounds produced within the healing tissues in response to wounding stress are polar in nature, consistent with prior reports that resistance to infection directly after tuber wounding is related to the appearance of phenolic monomers that subsequently serve as substrates for suberin polyphenolic biosynthesis.[34] The increase in antioxidant activity for nonpolar extracts as healing progresses from day 3 to 7 is in contrast with our observations for the polar portions, which tend to maintain their antioxidant activity levels, except for the Yukon Gold cultivar (Figures 4B and D).[4]

In addition, the $ABTS^{\bullet+}$ assay allows us to evaluate the capacity of both fast- and slow-acting antioxidants.[32] The TEAC values displayed in Figure 4 for both 3- and 7-day time points show overall increases in antioxidant activity throughout the assay period (0−45 min). This trend, which parallels observations made for the corresponding polar tissue extracts,[12] demonstrates the presence of both fast- and slow-acting antioxidants. Finally, the absence of steric hindrance in the $ABTS^{\bullet+}$ assay allows sampling of the scavenging activity of substances with diverse molecular weights and architectural features.[32,33]

Solid-State NMR Tracks Postwounding Development of Suberin Biopolymers. A stacked plot of the quantitatively reliable multi-CP MAS ^{13}C NMR spectra for solid interfacial layers from the four day-7 wound-healing tissues shows largely

DOI: 10.1021/acs.jafc.5b03206
J. Agric. Food Chem. 2015, 63, 6810−6822

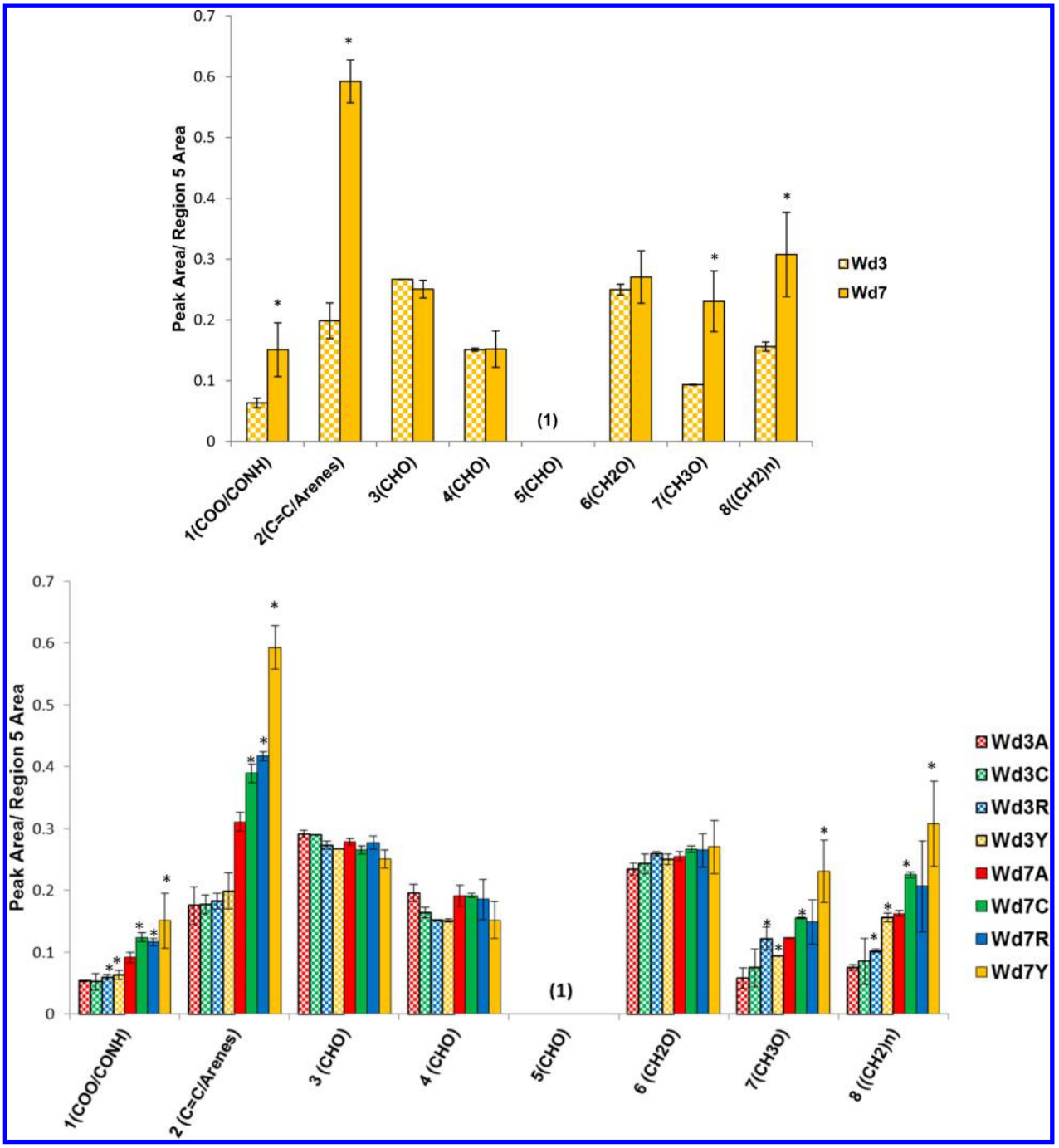

Figure 6. Peak ratios from 150 MHz multi-CP MAS ^{13}C NMR spectra for the solid interfacial layer from suberin-enriched potato wound-healing samples of the Yukon Gold cultivar (top) and all four cultivars (bottom) at days 3 (Wd3) and 7 (Wd7) postwounding, calculated with respect to the major polysaccharide CHO peaks in region 5 (67−80 ppm). The samples are coded for Atlantic (red, A), Chipeta (green, C), Norkotah Russet (blue, R), and Yukon Gold (gold, Y). The data represent the mean ± standard error of the mean of two biological replicates. Asterisks (*) are used to denote the most significant differences in peak area ratio with respect to day 3 (top) and with respect to Atlantic at any wounding time point (bottom) ($P < 0.05$, from Tukey pairwise comparisons).[21]

concordant chemical shifts but clear differences in relative peak intensities (Figure 5). The spectra of the suberin samples at day 7 are similar in appearance to those obtained from the day-7 wound periderm in prior studies of potato tubers.[19,35] (A unique peak at 198 ppm in the Yukon day-7 sample is attributable to a carbonyl within an aldehyde group.) Because quantitative comparisons *between* spectra of different plant materials can be skewed by inconsistencies in mass and instrumental conditions,[36] relative peak ratios *within* each spectrum were used to make compositional comparisons of the interfacial solids at each time point after wounding; the resulting trends were then interpreted in conjunction with metabolomic analyses of the soluble periderm extracts. Illustrative comparisons were made with respect to the major polysaccharide CHO group (region 5; Figure 6) and to the suberin carboxyl/amide groups (region 1; Figure 7).

With respect to the Yukon Gold polysaccharides (region 5), the integrated peak areas of the carboxyl/amide (region 1),

DOI: 10.1021/acs.jafc.5b03206
J. Agric. Food Chem. 2015, 63, 6810−6822

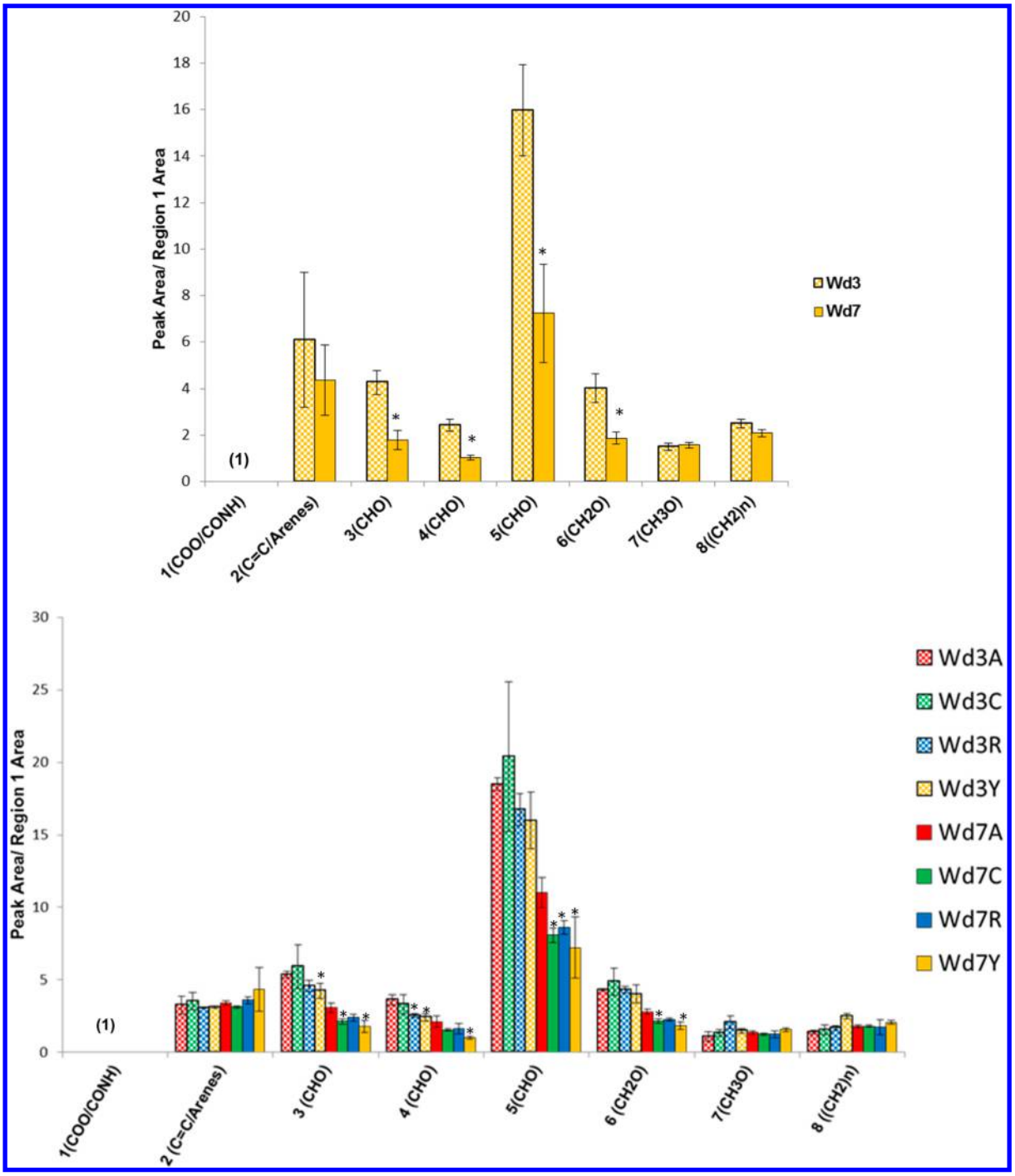

Figure 7. Peak ratios from 150 MHz multi-CP MAS ^{13}C NMR spectra for the solid interfacial layer from suberin-enriched potato wound-healing samples of the Yukon Gold cultivar (top) and all four cultivars (bottom) at days 3 (Wd3) and 7 (Wd7) postwounding, calculated with respect to the carbonyl peak in region 1 (168−180 ppm). The samples are coded for Atlantic (red, A), Chipeta (green, C), Norkotah Russet (blue, R), and Yukon Gold (gold, Y). The data represent the mean ± standard error of the mean of two biological replicates. Asterisks (*) are used to denote the most significant differences in peak area ratio with respect to day 3 (top) and with respect to Atlantic at any wounding time point (bottom) ($P < 0.05$, from Tukey pairwise comparisons).[21]

aromatic/alkene (region 2), methoxy (region 7), and chain methylene groups (region 8) increase significantly at day 7 compared with day 3 postwounding (Figure 6, top). Similar trends are observed for all cultivars (Figure 6, bottom). The relative increase in methylene peak areas for the interfacial layers at day 7 indicates increased hydrophobicity of the wound tissue, which should result in better protection against water loss. The increase in the ratio of methylene chain compounds ($(CH_2)_n$, region 8) is also in accord with the potential marker compounds identified above primarily in day-7 nonpolar extracts, which are mostly compounds containing long-chain aliphatic moieties. Analogously, the increases in peak area ratios involving the carboxyls/amides (COO/CONH, region 1), aromatics (C═C/arenes, region 2), and methoxy groups (CH_3O, region 7) align with the findings of amide-, methoxy-, and carboxyl-containing phenolic markers in our polar wound-

DOI: 10.1021/acs.jafc.5b03206
J. Agric. Food Chem. 2015, 63, 6810−6822

healing tissue extracts.[12] These latter markers include phenolic acids and phenolic amines, including derivatives of ferulic acid that become more abundant at day 7. Moreover, the larger aromatic-to-CHO ratios observed in day-7 Yukon Gold suberin samples (Figures 6) fit with trends observed for the marker compounds in the polar extracts: an increased number of aromatic markers is detected for this cultivar.[12] Together, these correlations suggest that both nonpolar and polar[4] soluble compounds can be viewed as precursors of the suberized cell wall layer that is being formed during the healing process.

At the day-7 time point, when the wound periderm layer is forming, peak area ratios for carboxyl/amide (COO/CONH, region 1), aromatic/alkene (C═C/arenes, region 2), methoxy (CH_3O, region 7), and chain methylene ($(CH_2)_n$, region 8) groups are found to be the highest in Yukon Gold and lowest in Atlantic (Figure 6, bottom, and Figure S2). This observation suggests that the suberin formed in Yukon Gold at day 7 has a higher proportion of long-chain aliphatic compounds, which can provide increased hydrophobicity and lead to decreased water permeability. The small ratio of COO/CONH groups with respect to polysaccharides observed for Atlantic also supports the hypothesis of diminished suberization that was proposed from analysis of the nonpolar soluble marker compounds.

When measured with respect to the carboxyl/amide signals (region 1), the integrated peak areas for oxygenated aliphatic compounds in regions 3−6 are found to decrease for all cultivars between day 3 and day 7 (Figure 7). This trend supports and extends the ratios outlined above: whereas (region 5)/(region 1) is just the inverse of the carbonyl-to-CHO ratio, additional polysaccharide peak areas in regions 3, 4, and 6 also decrease with respect to the suberin esters and amides that contribute to region 1 of the spectrum. Thus, these latter results reinforce the conclusion that deposition of the aliphatic-aromatic suberin polyester within the phellem cell-wall tissues during development of the wound periderm diminishes the polysaccharide-to-fatty acyl ester ratio. As noted above, the relative increase in carbonyl, aromatic, and olefinic groups can be related to both soluble polar and nonpolar potential marker compounds, many of which contain these functional groups. At day 7, Yukon has the lowest and Atlantic the highest peak area ratios for each of the oxygenated aliphatics in regions 3−6 (Figure 7 and Figure S3).

It is also notable that, among the suberin-associated groups, the aromatic/alkene moieties (C═C/arenes, region 2) show the most dramatic increase in relative intensity with respect to the polysaccharide carbons (Figure 6). This finding suggests that the majority of the compounds being deposited in the polyphenolic domain of suberin during the 3-to-7 day time frame originate from the polar extracts, as this is the layer that is rich in aromatic and olefinic structures (phenolic amines, flavonoids, and phenolic acids).[4]

Coordinated Measurements Provide a Chemical Picture of Potato Tuber Wound Healing. GC/MS multivariate analysis shows convergence of the nonpolar soluble metabolite composition at the day-7 time point after wounding of the potato tubers, suggesting induction of a common biosynthetic pathway as a result of wounding and suberization in all four cultivars. A similar trend was observed among the potential polar markers.[12] Analysis of the GC/MS data leads to the identification of 28 potential cultivar-specific and wound-healing marker compounds that discriminate among cultivar types and between wound healing time points day 3 and 7, during closing layer and periderm development. The distribution of nonpolar soluble markers (Figure 3) dovetails with the trends observed in the solid suberin composition of the cultivars at the same time point (Figures 6 and 7). That is, at day 7, Yukon Gold has the highest and Atlantic has the lowest relative amount of solid chain methylene-containing compounds in their respective suberin samples. This observation parallels the trend among the soluble nonpolar fatty acid markers (Figure 3B, Table 2), which at day 3 display the highest number of long-chain and very-long-chain homologues for Yukon Gold but at day 7 are diminished and putatively undergoing incorporation into the solid suberin biopolymer. It is sensible to propose, then, that the hydrocarbon chains of the fatty acid compounds contribute to the solid-state ^{13}C NMR resonance corresponding to the long-chain aliphatic suberin constituents. Conversely, the nonpolar extracts from the Atlantic cultivar exhibit no day-3 markers from these two classes or from glyceryl esters. The paucity of glyceryl esters, dioic acids, and hydroxyfatty acids in nonpolar Atlantic extracts, when considered in conjunction with the lowered proportions of COO/CONH groups in the interfacial solids, suggest a diminished extent of suberization.

For the solid suberized tissues (Figure 7), elevated ratios of methylene chain-containing compounds in the wound-healing tissues of all cultivars at day 7 can increase the periderm hydrophobicity, thereby offering the potential for more protection against water loss. The presence of flavonoid, phenolic acid, and phenolic amine marker compounds, all of which contain carboxyl or amide groups, in the polar extracts at both day-3 and day-7 time points, could also correlate with the deposition of such carbonyl-containing compounds in the Yukon Gold suberin at both time points.[12] The most vigorous deposition of alkenes and arenes at day 7, which is observed for Yukon Gold suberin samples (Figures 6 and 7), is in accord with trends observed among the aromatic markers found in the polar extracts of this cultivar.[12] Nonetheless, we note that rigorous validation of the metabolite profiling and solid-state NMR results for various cultivars at different wound-healing time points would require consideration of cultural, environmental, and geographic factors. A large-scale study including additional earlier and later wound-healing time points would also provide greater insight into these dynamic changes.

The antioxidant results show definitively that the scavenging activities of the nonpolar wound tissue extracts are 50−100 times smaller than those of the corresponding polar extracts, for each time point and for all four cultivars (Figure 4). Therefore, it can be concluded that the majority of the antioxidant compounds produced in the wound tissues are polar compounds, such as phenolic acids and flavonoids. At both day 3 and day 7, the nonpolar extract of Norkotah Russet demonstrated the highest antioxidant activity, an observation that can be attributed to the presence of unsaturated fatty acids among its potential markers. Among the nonpolar metabolite markers are compounds that may offer protection against invasion by plant pathogens based on their previous antimicrobial activity reported in vitro. They include unsaturated fatty acids, oleic acid (**15**, 18:1) and linoleic acid (**17**, 18:2); saturated fatty acids, tetradecanoic acid (**14**, 14:0) and hexadecanoic acid (**12**, 16:0); and the diacid azaleic acid (**5**, 9:0). In addition, we have previously identified marker compounds in polar extracts of the wound tissues that include phenolic amines, glycoalkaloids, flavonoids and phenolic acids, for which in vitro antimicrobial, insecticidal, and antioxidant

DOI: 10.1021/acs.jafc.5b03206
J. Agric. Food Chem. 2015, 63, 6810−6822

properties have been reported and which might offer protection to the wounded tuber surface.[12,37,38] Thus, the chemical picture of the defensive armor of the potato tuber that emerges from the current study encompasses both polar and nonpolar metabolites that may possess antimicrobial, antioxidant, and insecticidal properties and also the solid suberin biopolymer, which can provide robust defensive barriers in diverse cultivars.

■ ASSOCIATED CONTENT

Supporting Information

Table of metabolites, statistical analysis results. The Supporting Information is available free of charge on the ACS Publications website at DOI: 10.1021/acs.jafc.5b03206.

■ AUTHOR INFORMATION

Corresponding Author

*Phone: +1 212 650 8916. E-mail: stark@sci.ccny.cuny.edu.

Funding

Financial support for this work was obtained from the U.S. National Science Foundation (NSF MCB-0843627, 1411984, and 0741914 to R.E.S.), a PSC−CUNY Grant from the City University of New York (TradA-45-367 to V.C.P.), and a mobility grant from the Spanish Ministry of Education (JC2010-0147 to O.S.). The NMR resources were supported by The City College of New York (CCNY) and the CUNY Institute of Macromolecular Assemblies, with infrastructural assistance provided by the National Institutes of Health through the National Center for Research Resources (2G12RR03060) and National Institute on Minority Health and Health Disparities (8G12 MD007603). The GC/MS instrument was supported by NSF (CHE-0840498).

Notes

The authors declare no competing financial interest.

■ ACKNOWLEDGMENTS

Joe Nuñez (University of California Cooperative Extension) supplied the potato tubers for analysis. The authors would like to acknowledge Dr. Hsin Wang, Cristina Veresmortean, and Boris Kalmatsky for their valuable technical assistance with the NMR and GC/MS instruments. We thank Oseloka Chira for his diligent work in processing the NMR data. Professor David Jeruzalmi provided generous access to the microplate reader.

■ ABBREVIATIONS USED

ABTS$^{\bullet+}$, 2,2′-azinobis (3-ethylbenzothiazoline-6-sulfonic acid ammonium salt) free radical; CPMAS, cross-polarization magic-angle spinning; DPMAS, direct polarization magic-angle spinning; MSTFA, *N*-methyl-*N*-(trimethylsilyl)-trifluoroacetamide; OPLS-DA, orthogonal partial least-squares discriminate analysis; PCA, principal component analysis; TMCS, trimethylchlorosilane

■ REFERENCES

(1) Varns, J. L.; Schaper, L. A.; Preston, D. A. Potato losses during the first three months of storgae for processing. *Am. Potato J.* **1985**, *62*, 91−99.

(2) Franke, R.; Schreiber, L. Suberin- a biopolyester forming apoplastic plant interfaces. *Curr. Opin. Plant Biol.* **2007**, *10*, 252−259.

(3) Beisson, F.; Li-Beisson, Y.; Pollard, M. Solving the puzzles of cutin and suberin polymer biosynthesis. *Curr. Opin. Plant Biol.* **2012**, *15*, 329−337.

(4) Bernards, M. A. Demystifying suberin. *Can. J. Bot.* **2002**, *80*, 227−240.

(5) Mattinen, M.-L.; Filpponen, I.; Järvinen, R.; Li, B.; Kallio, H.; Lehtinen, P.; Argyropoulos, D. Structure of the polyphenolic component of suberin isolated from potato (*Solanum tuberosum* var. Nikola). *J. Agric. Food Chem.* **2009**, *57*, 9747−9753.

(6) Graça, J.; Santos, S. Suberin: A biopolyester of plant's skin. *Macromol. Biosci.* **2007**, *7*, 128−135.

(7) Järvinen, R.; Silvestre, A. J. D.; Holopainen, U.; Kaimainen, M.; Nyyssölä, A.; Gil, A. M.; Pascoal Neto, C.; Lehtinen, P.; Buchert, J.; Kallio, H. Suberin of potato (Solanum tuberosum var. Nikola): Comparison of the effect of cutinase CcCut1 with chemical depolymerization. *J. Agric. Food Chem.* **2009**, *57*, 9016−9027.

(8) Yang, W.-L.; Bernards, M. A. Metabolite profiling of potato (*Solanum tuberosum* L.) tubers during wound-induced suberization. *Metabolomics* **2007**, *3*, 147−159.

(9) Neubauer, J. D.; Lulai, E. C.; Thompson, A. L.; Suttle, J. C.; Bolton, M. D. Wounding coordinately induces cell wall protein, cell cycle and pectin methyl esterase genes involved in tuber closing layer and wounding periderm development. *J. Plant Physiol.* **2012**, *169*, 586−595.

(10) Lulai, E. C.; Corsini, D. L. Differential deposition of suberin phenolic and aliphatic domains and their roles in resistance to infection during potato tuber (*Solanum tuberosum* L.) wound healing. *Physiol. Mol. Plant Pathol.* **1998**, *53*, 209−222.

(11) Yang, W.-L.; Bernards, M. A. Wound-induced metabolism in potato (*Solanum tuberosum*) tubers. *Plant Signaling Behav.* **2006**, *1*, 59−66.

(12) Dastmalchi, K.; Cai, Q.; Zhou, K.; Huang, W.; Serra, O.; Stark, R. E. Solving the Jigsaw puzzle of wound-healing potato cultivars: Metabolite profiling and antioxidant activity of polar extracts. *J. Agric. Food Chem.* **2014**, *62*, 7963−7975.

(13) Choi, H.-K.; Choi, Y. H.; Verberne, M.; Lefeber, A. W. M.; Erkelens, C.; Verpoorte, R. Metabolic fingerprinting of wild type and transgenic tobacco plants by ^{1}H NMR and multivariate analysis technique. *Phytochemistry* **2004**, *65*, 857−864.

(14) Kim, H. K. C.; Choi, Y. H.; Verpoorte, R. NMR-based metabolomic analysis of plants. *Nat. Protoc.* **2010**, *5*, 536−549.

(15) Katajamaa, M.; Miettinen, J.; Orešič, M. MZmine: Toolbox for processing and visualization of mass spectrometry based molecular profile data. *Bioinformatics* **2006**, *22*, 634−636.

(16) Worley, B.; Powers, R. Multivariate analysis in metabolomics. *Curr. Metabol.* **2013**, *1*, 92−107.

(17) Wiklund, S., Multivariate Data Analysis and Modelling in "Omics". Umetrics AB: San Jose, CA, 2008.

(18) Fung, B. M.; Khitrin, A. K.; Ermolaev, K. An improved broadband decoupling sequence for liquid crystals and solid. *J. Magn. Reson.* **2000**, *142*, 97−101.

(19) Serra, O.; Chatterjee, S.; Figueras, M.; Molinas, M.; Stark, R. E. Deconstructing a plant macromolecular assembly: Chemical architecture, molecular flexibility, and mechanical performance of natural and engineered potato suberins. *Biomacromolecules* **2014**, *15*, 799−811.

(20) Johnson, R. L.; Schmidt-Rohr, K. Quantitative solid-state ^{13}C NMR with signal enhancement by multiple cross polarization. *J. Magn. Reson.* **2014**, *239*, 44−49.

(21) Jackson, S. *Research methods: A modular approach*; Cengage Learning: Stamford, CT, 2014; p 316−317.

(22) Quintanilla-Licea, R.; Morado-Castillo, R.; Gomez-Flores, R.; Laatsch, H.; Verde-Star, M. J.; Hernández-Martínez, H.; Tamez-Guerra, P.; Tamez-Guerra, R.; Rodríguez-Padilla, C. Bioassay-guided isolation and identification of cytotoxic compounds from *Gymnospera glutinosum* leaves. *Molecules* **2012**, *17*, 11229−11241.

(23) Liu, S.; Ruan, W.; Li, J.; Xu, H.; Wang, J.; Gao, Y.; Wang, J. Biological control of phytopathogenic fungi by fatty acids. *Mycopathologia* **2008**, *166*, 93−102.

(24) Ginzberg, I. Wound-periderm formation. In *Induced plant resistance to Herbivory*, Schaller, A., Ed. Springer: Berlin, 2008.

(25) Walters, D.; Raynor, L.; Mitchell, A.; Walker, R.; Walker, K. Antifungal activities of four fatty acids against plant pathogenic fungi. *Mycopathologia* **2004**, *157*, 87−90.

DOI: 10.1021/acs.jafc.5b03206
J. Agric. Food Chem. 2015, 63, 6810−6822

(26) Wang, W.; Tian, S.; Stark, R. E. Isolation and identification of triglycerides and ester oligomers from partial degradation of potato suberin. *J. Agric. Food Chem.* **2010**, *58*, 1040−1045.
(27) Jung, H. W.; Tschaplinski, T. J.; Wang, L.; Glazebrook, J.; Greenberg, J. T. Priming in systemic plant immunity. *Science* **2009**, *324*, 89−91.
(28) Schreiber, L.; Franke, R.; Hartmann, K. Wax and suberin development of native and wound periderm of potato (*Solanum tuberosum*) and its relation to peridermal transpiration. *Planta* **2005**, *220*, 520−530.
(29) Řezanka, T.; Sigler, K. Odd-numbered very-long-chain fatty acids from the microbial, animal and plant kingdoms. *Prog. Lipid Res.* **2009**, *48*, 206−238.
(30) Reyes, L. F.; Villarreal, J. E.; Cisneros-Zevallos, L. The increase in antioxidant capacity after wounding depends on the type of fruit or vegetable tissue. *Food Chem.* **2007**, *101*, 1254−1262.
(31) Reyes, L. F.; Cisneros-Zevallos, L. Wounding stress increases the phenolic content and antioxidant capacity of purple-flesh potatoes (*Solanum tuberosum* L.). *J. Agric. Food Chem.* **2003**, *51*, 5296−5300.
(32) Prior, R. L.; Wu, X.; Schaich, K. Standardized methods for the determination of antioxidant capacity and phenolics in foods and dietary supplements. *J. Agric. Food Chem.* **2005**, *53*, 4290−4302.
(33) Magalhães, L. M.; Segundo, M. A.; Reis, S.; Lima, J. L. F. C. Methodological aspects about in vitro evaluation of antioxidant properties. *Anal. Chim. Acta* **2008**, *613*, 1−19.
(34) Lulai, E. C., Skin-set, wound-healing, and related defects. In *Potato biology and biotechnology. Advances and Perspectives*, 1st ed.; Vreugdenhil, D.; Bradshaw, J.; Gebhardt, C.; Govers, F.; Mackerron, D. K. L.; Taylor, M. A.; Ross, H. A., Eds.; Elsevier: Oxford, UK, 2007; pp 471−500.
(35) Yan, B.; Stark, R. E. Biosynthesis, molecular structure, and domain architecture of potato suberin: A ^{13}C NMR study using isotopically labeled precursors. *J. Agric. Food Chem.* **2000**, *48*, 3298−3304.
(36) Kolodziejski, W.; Klinowski, J. Kinetics of cross-polarization in solid-state NMR: A guide for chemists. *Chem. Rev.* **2002**, *102*, 613−628.
(37) Back, K. Hydroxycinnamic acid amides and their possible utilization for enhancing agronomic traits. *Plant Pathology J.* **2001**, *17*, 123−127.
(38) Milner, S. E.; Brunton, N. P.; Jones, P. W.; O' Brien, N. M.; Collins, S. G.; Maguire, A. R. Bioactivities of glycoalkaloids and their aglycones from *Solanum tuberosum*. *J. Agric. Food Chem.* **2011**, *59*, 3454−3484.

DOI: 10.1021/acs.jafc.5b03206
J. Agric. Food Chem. 2015, 63, 6810−6822